

Cavendish-HEP-95/15

DFTT 04/95

DTP/95/10

May 1996

## Perturbative rates and colour rearrangement effects in four-jet events at LEP2

A. Ballestrero<sup>a</sup>, V.A. Khoze<sup>b</sup>, E. Maina<sup>a</sup>,  
S. Moretti<sup>a,c</sup> and W.J. Stirling<sup>b,d</sup>

*a) Dipartimento di Fisica Teorica, Università di Torino,  
and I.N.F.N., Sezione di Torino,  
Via Pietro Giuria 1, 10125 Torino, Italy.*

*b) Department of Physics, University of Durham,  
South Road, Durham DH1 3LE, UK.*

*c) Cavendish Laboratory, University of Cambridge,  
Madingley Road, Cambridge CB3 0HE, UK.*

*d) Department of Mathematical Sciences, University of Durham,  
South Road, Durham DH1 3LE, UK.*

### Abstract

An important issue in the direct reconstruction method of determining the  $W$  mass from  $q\bar{q}Q\bar{Q}$  events at LEP2 concerns the impact of the relatively unknown QCD interconnection effects. It has been suggested that a study of ‘short string’ states, in which colour singlet states are formed from  $q\bar{Q}$  and  $Q\bar{q}$  pairs with small phase-space separation, could shed important light on this issue. We show that such configurations can also be generated by conventional background  $e^+e^- \rightarrow 4$  parton processes, in particular QCD  $q\bar{q}gg$  and  $q\bar{q}Q\bar{Q}$  and non-resonant electroweak  $q\bar{q}Q\bar{Q}$  production. We study the colour and kinematic structure of these background contributions, and estimate the event rate to be expected at LEP2. We find that the QCD processes are heavily suppressed, but that non-resonant  $q\bar{q}Q\bar{Q}$  production may be comparable in rate to the expected ‘short string’ signal from  $W^+W^-$  production.

# 1 Introduction

The detailed study of  $W^\pm$  boson physics is one of the most important goals of the LEP2  $e^+e^-$  collider. Among the main objectives is a precision measurement of the mass  $M_W$  of the  $W$  boson, with the target accuracy  $\pm 50$  MeV, see for example Ref. [1].

An obvious requirement for the success of these precise studies is a high level of reliability of theoretical predictions for the signal and background contributions to various experimental observables related to the different methods of measuring  $M_W$  from the process  $e^+e^- \rightarrow W^+W^-$ . This, in particular, requires a detailed understanding of the physical phenomena which describe the production and decay of  $W^\pm$  bosons at LEP2, for instance, of the effects which arise from the relatively large  $W^\pm$  boson decay width  $\Gamma_W$  ( $\simeq 2.1$  GeV [2]). The instability of the  $W^\pm$  bosons can, in principle, strongly modify the standard ‘stable  $W^\pm$ ’ results. For example, an important role can be played by QCD radiative interferences (both virtual and real) which interconnect the production and decay stages, see for example Refs. [3, 4].

It is currently believed that the highest precision on the  $M_W$  determination is obtained from the method of direct kinematic reconstruction of  $M_W$  using the decay channels<sup>1</sup>

$$W^+W^- \rightarrow q_1\bar{q}_2Q_3\bar{Q}_4, \quad (1)$$

$$W^+W^- \rightarrow q\bar{q}\ell\nu_\ell. \quad (2)$$

However, the direct reconstruction method is not without problems. For example, to construct the two  $W^\pm$ ’s from the  $q_1\bar{q}_2Q_3\bar{Q}_4$  final state in (1) one must, in principle, attribute all observed hadrons to the ‘correct’ parent  $W^\pm$ , a procedure which is certainly affected by relatively unknown QCD interconnection corrections [4]. Since a complete description of these effects is not possible at present, one has to rely on model predictions rather than on exact calculations, for details see Refs. [1, 4, 5, 6, 7]. Detailed experimental studies of four-jet events in  $e^+e^-$  annihilation corresponding to the kinematics of process (1) could provide important information about the size of interconnection-related systematic uncertainties in the  $W$  mass measurements.

There is another challenging reason to study carefully the phenomenon of QCD interconnection (colour rearrangement) in hadronic  $W^+W^-$  events. As first emphasised in

---

<sup>1</sup>We use the notation  $q$  and  $Q$  to distinguish quarks from different  $W$  decay.

Ref. [8], it could provide a new laboratory for probing non-perturbative QCD dynamics. The fact that different models for the non-perturbative fragmentation give different predictions [1] means that it might be possible to learn about the structure of the QCD vacuum. For example, one may hope to distinguish various scenarios by exploiting the difference in the sensitivity of the reconnection to the event topology [4, 5].

Unfortunately to make any progress at all, we have so far had to rely on models and approximations that are far from perfect. There is a true limit to our current physics understanding. One unresolved problem concerns an evident breakdown of the exclusive probabilistic interpretation of the colour suppressed interference effects, see Refs. [2, 4].

Recall that there is an important difference between the perturbative QCD ‘radio-physics’ picture [9] and the non-perturbative fragmentation scenarios like, for example, the Lund string model [10]. The latter requires a completely exclusive description: in the end the  $q_1\bar{q}_2Q_3\bar{Q}_4$  system must be subdivided into and fragment as two separate colour singlets, either  $q_1\bar{q}_2$  and  $Q_3\bar{Q}_4$  or  $q_1\bar{Q}_4$  and  $Q_3\bar{q}_2$ . The string model therefore predicts effects that could be observed on an event-by-event basis. On the other hand, within the perturbative QCD approach, analogously to other colour suppressed interference effects [9, 11, 12], the colour rearrangement phenomena can be viewed only on a completely inclusive basis, when all the antennae/dipoles are simultaneously active in the particle production. The fact that the reconnection pieces are not positive-definite [4] reflects their wave interference nature. Therefore, the recoupling effects should appear on top of a background generated by standard no-reconnection antennae/colour dipoles. Normally (for example, for  $e^+e^- \rightarrow q\bar{q}g$ ) the two pictures give quite similar overall description; differences only become dramatic when dealing with small colour suppressed effects, see Refs. [9, 11, 12]. Another open question concerns the interplay between the perturbative and non-perturbative phases in the reconnection [4].

The issue of the experimental observability of colour reconnection needs a special detailed consideration. For example, in Ref. [4] the analysis was concerned mainly with the standard global event measures where the effects appear to be very small. The change in the average charged multiplicity is predicted at a level of a percent or less, and similar conclusions hold for rapidity distributions, thrust distributions, and so on. This is very likely below the experimental precision one may expect at LEP2, and so the effects may well be unobservable. There are, however, some other potentially promising approaches, e.g. the comparison of the event properties in fully hadronic and mixed leptonic-hadronic decays

or the comparison with measurements from the  $p\bar{p}$  collider, see for example Refs. [2, 4]. In particular, an interesting vista on the reconnection issue is provided by Bose–Einstein effects [13].

A high–statistics run above the  $Z^0 Z^0$  threshold would of course allow an unambiguous determination of any systematic mass shift, since the  $Z^0$  mass is already very precisely known from LEP1. If the various potential sources of systematic error could be disentangled, it could also provide a direct observation of reconnection effects. More generally,  $Z^0$  events from LEP1 could be used to predict a number of properties for  $Z^0 Z^0$  events, such as the charged multiplicity distribution. Any sign of deviations would then provide important information on the reconnection issue.

An interesting proposal which attempts to disentangle the recoupling phenomenon is discussed in Ref. [5], where it is argued that dynamical effects could enhance the reconnection probability for configurations which correspond to so–called ‘short strings’, i.e. strings connecting  $q_1$  with  $\bar{Q}_4$  (and  $\bar{q}_2$  with  $Q_3$ ) when the quark–antiquark pairs are close together in phase space, equivalently, when the event has a high thrust. Such configurations would be expected to produce fewer hadrons than average. It is estimated that with 10% probability for recoupling these reconnected events could be experimentally identified.

However, in order to clearly pin down such a manifestation of colour rearrangement in process (1) in a realistic LEP2 scenario further effort is required. One of the most important questions concerns the size of the non– $W^+W^-$  background. For example, the ‘short string’ states discussed above can also be generated by conventional  $e^+e^- \rightarrow 4$  parton events in specific colour configurations which give rise to ‘rapidity gaps’, see Refs. [14, 15, 16, 17]. Such events provide a natural lower limit for a recoupling–type signal<sup>2</sup>.

In this study we calculate all the four–parton background contributions which could give events with large rapidity gaps. We use the exact lowest–order tree–level matrix elements to compute the overall four–jet cross sections, and then study the colour and kinematic structure of the various processes. In this way we are able to estimate the probability of finding background configurations corresponding to two pairs of partons in colour singlet states and relatively close together in phase space, configurations which could give rise to rapidity gaps.

The paper is organised as follows. In the following section we list the various signal

---

<sup>2</sup>We assume here that these rapidity gap events would be statistically distinguishable from random fluctuations in conventional  $e^+e^- \rightarrow 2$  jet production

and background four-parton processes and discuss their colour properties. In Section 3 we present numerical studies of the corresponding cross sections at LEP2 energies. Our conclusions are presented in Section 4.

## 2 Recoupled four-jet events

As discussed in the Introduction, a natural lower limit for the colour recoupling signal in  $W^+W^-$  hadronic events is provided by  $e^+e^- \rightarrow 4$  partons background events with sufficiently large rapidity gaps [14, 15, 16, 17]. One can expect that when the two colour singlet quasi-collinear jet pairs are moving apart in the centre-of-mass frame with large velocities, the production of hadrons is suppressed in the rapidity region separating the two colour singlet systems. Therefore these rapidity gap events can, in principle, mimic the ‘short string’ signal of the  $W^+W^-$  hadronic events advocated in Ref. [5] (see also [8]) as a laboratory for studying colour recoupling effects.<sup>3</sup> Note that contrary to the  $W^+W^-$  case, where the ‘short string’ signal is suppressed by a small (but theoretically uncertain) recoupling factor, four partons in a rapidity gap configuration are produced almost simultaneously in a small space-time interval, and so all the QCD antennae/dipoles are equally active. In addition, the soft and collinear singularities inherent in the QCD matrix elements imply that selecting four-jet events with a high thrust, which enhances the recoupling signal [5], automatically enhances the role of rapidity gap background events.

We would expect [14, 15] that the global features of rapidity gap events could be evaluated within the framework of perturbative QCD. We therefore base our analysis on the tree-level matrix elements for the following four-jet processes,

$$e^+e^- \rightarrow W^+W^- \rightarrow q_1\bar{q}_2Q_3\bar{Q}_4, \quad (3)$$

$$e^+e^- \rightarrow q_1\bar{q}_2g_3g_4, \quad (4)$$

$$e^+e^- \rightarrow q_1\bar{q}_2Q_3\bar{Q}_4 \quad (\text{via } g \text{ propagators}), \quad (5)$$

$$e^+e^- \rightarrow q_1\bar{q}_2Q_3\bar{Q}_4 \quad (\text{via } \gamma, Z^0 \text{ propagators}), \quad (6)$$

described by the Feynman diagrams<sup>4</sup> shown in Figs. 1–3. The matrix element for (3) is calculated using the techniques described in [18] while for (4)–(6) we use the same **FORT**TRAN

<sup>3</sup>Note also that the high thrust selection automatically selects a class of events in which QCD radiation from the final-state quarks is suppressed.

<sup>4</sup> $W^\pm$ -propagator contributions are omitted from the diagrams of Fig. 3a for process (6).

codes of Refs. [19, 20, 21], to which the reader can refer for details. The results obtained for process (3) have been cross-checked with a calculation using the formalism of Ref. [22].

Configurations corresponding to two distinctively separated colour singlet parton pairs, which should lead to rapidity gap events, are illustrated schematically in Fig. 4 for the processes (3)–(6) listed above: Fig. 4a for process (4) (see also Fig. 2), Fig. 4b for process (5) (see also Fig. 3a when the jagged line represents a  $g$ ), and Figs. 4c,d for processes (3) (4d only) and (6) (see also Fig. 1, Fig. 3a when the jagged line represents a  $\gamma$  or a  $Z^0$ , and Fig. 3b).

There is a simple heuristic way to derive the colour factors for the production of a  $q\bar{q}$  pair in a colour singlet ( $S$ ) or octet ( $O$ ) state. In terms of colour matrices, the production of a singlet state must be proportional to the identity and therefore:

$$\text{Diagram of } S \text{ state} = A_S \text{ Diagram of } S \text{ loop}$$

Here and in the following we will only draw the *colour part* of the full Feynman amplitudes. The production of a quark–antiquark pair in an octet state, on the other hand, must be proportional to the production of a gluon state:

$$\text{Diagram of } O \text{ state} = A_O \text{ Diagram of } O \text{ loop with gluon}$$

These equalities are exact, with  $A_S = 1/\sqrt{3}$  and  $A_O = \sqrt{2}$ , for all quark and gluon indices if, in the  $RGB$  colour basis, we use the usual Gell–Mann matrices and the following set of gluon states:  $g_1 = (R\bar{G} + G\bar{R})/\sqrt{2}$ ,  $g_2 = i(R\bar{G} - G\bar{R})/\sqrt{2}$ ,  $g_3 = (R\bar{R} - G\bar{G})/\sqrt{2}$ ,  $g_4 = (B\bar{R} + R\bar{B})/\sqrt{2}$ ,  $g_5 = i(B\bar{R} - R\bar{B})/\sqrt{2}$ ,  $g_6 = (G\bar{B} + B\bar{G})/\sqrt{2}$ ,  $g_7 = i(G\bar{B} - B\bar{G})/\sqrt{2}$ ,  $g_8 = (R\bar{R} + G\bar{G} - 2B\bar{B})/\sqrt{6}$ , with the singlet state given by  $g_0 = (R\bar{R} + G\bar{G} + B\bar{B})/\sqrt{3}$ . When computing colour traces only  $A_S^2$  and  $A_O^2$  are needed. These can also be obtained from the processes  $e^+e^- \rightarrow q\bar{q}$ , which can only result in a singlet state, and  $q_1\bar{q}_1 \rightarrow q_2\bar{q}_2$ ,

with  $q_1 \neq q_2$ , in which the initial and final quark pairs are necessarily in the octet state. One again finds  $A_S^2 = 1/3$  and  $A_O^2 = 2$ .

An alternative way to obtain the same results is to recall the identity, see for example Ref. [9],

$$T_{ij}^a T_{kl}^a = \frac{1}{2} \left( \delta_{il} \delta_{jk} - \frac{1}{3} \delta_{ij} \delta_{kl} \right) \quad (7)$$

which graphically reads:

By multiplying by two and isolating the first term on the right-hand side, which represents a generic  $q\bar{q}$  state, it is straightforward to show that the coefficients of the singlet and octet terms are exactly  $A_S^2$  and  $A_O^2$  respectively.

Using these simple calculational tools one can compute the colour factors for the production of  $q\bar{q}$  pairs in the singlet state for all the above four-jet processes in  $e^+e^-$  collisions. It is sufficient to join the quark and antiquark *colour lines* in the amplitude and then to compute the colour factor for the amplitude squared with the usual rules, dividing the final result by three. Each of the processes under consideration is discussed in turn below.

- $e^+e^- \rightarrow W^+W^- \rightarrow q\bar{q}Q\bar{Q}$ ,  $q \neq Q$ . The colour factor is 9. If  $q\bar{q}(Q\bar{Q})$  are in a singlet state the colour factor is 1, if they are in an octet state it is 8. Therefore the colour rearrangement probability is  $1/9$ , as is well known. Similarly, the colour factors for  $e^+e^- \rightarrow q\bar{q}Q\bar{Q}$  via electroweak interactions (EW),  $q \neq Q$ , with  $q\bar{Q}$  in a singlet or octet state are 1 and 8 respectively.
- $e^+e^- \rightarrow q\bar{q}Q\bar{Q}$  via EW,  $q = Q$ . The full amplitude includes two sets of diagrams. The corresponding spinor parts are  $A_1$  and  $A_2$  which are related by the exchange of the momenta, for example, of the two antiquarks:

$$A = A_1 \begin{array}{c} \nearrow 1 \\ \searrow 2 \\ \nearrow 3 \\ \searrow 4 \end{array} - A_2 \begin{array}{c} \nearrow 1 \\ \searrow 2 \\ \nearrow 3 \\ \searrow 4 \end{array}$$

If we require the (12)-pair to form a colour singlet, the colour factors for the modulus squared of  $A_1$  and  $A_2$  are 9 and 1 respectively, and the colour factor for the interference between  $A_1$  and  $A_2$  is 3. The roles of  $A_1$  and  $A_2$  are obviously interchanged if instead we require the (13)-pair to form a colour singlet.

- $e^+e^- \rightarrow q\bar{q}Q\bar{Q}$  via QCD,  $q \neq Q$ . For the  $\mathcal{O}(\alpha^2\alpha_s^2)$  tree-level diagrams the  $q\bar{q}$  and  $Q\bar{Q}$  pairs are always in the octet state. The colour factor is 2. When  $q\bar{Q}$  form a singlet the colour factor is 16/9, and when they form an octet the colour factor is 2/9. In this case the probability of finding the  $q\bar{Q}$  pair in a singlet state is 8/9.
- $e^+e^- \rightarrow q\bar{q}Q\bar{Q}$  via QCD,  $q = Q$ . The corresponding amplitude includes two sets of four diagrams (only one is shown for simplicity) which are related by the exchange of the momenta, for example, of the two antiquarks:

$$A = A_1 \begin{array}{c} \begin{array}{c} \rightarrow 1 \\ \rightarrow 2 \\ \leftarrow 3 \\ \leftarrow 4 \end{array} \\ \text{diagram with gluon exchange} \end{array} - A_2 \begin{array}{c} \begin{array}{c} \rightarrow 1 \\ \rightarrow 2 \\ \leftarrow 4 \\ \leftarrow 3 \end{array} \\ \text{diagram with gluon exchange} \end{array}$$

If we require the (14) pair to form a colour singlet then only  $A_2$  contributes and the corresponding colour factor is 16/9. The roles of  $A_1$  and  $A_2$  are obviously interchanged if we require the (13) pair to form a colour singlet instead.

- $e^+e^- \rightarrow q\bar{q}gg$ . It is convenient to consider separately the orthogonal contributions which are symmetric (i.e. proportional to  $\{T^a, T^b\}/2$ ) and antisymmetric (i.e. pro-



portional to  $[T^a, T^b]/2$ ) in the gluon colour indices. The two quarks in the antisymmetric term can only be in the octet state. The colour factor is then 12. The colour factor for the symmetric part is  $28/3$ : when the quark pair is in the singlet state the colour factor is  $8/3$ , and when the pair is in the octet state the colour factor is  $20/3$ . Therefore in kinematic configurations for which the symmetric and antisymmetric amplitudes are approximately equal, the colour singlet pair configurations are suppressed by a factor  $\frac{1}{N_c^2-1} = \frac{1}{8}$ . In particular, configurations which correspond to colour singlet pairs in opposite hemispheres, which form the background to the  $W^+W^-$  ‘short string’ signal, are colour suppressed.

This last result highlights an important difference in principle between the treatment of rapidity gap events in the four-quark processes (5)–(6) and the double gluon bremsstrahlung process (4). In the former case two singlet pairs are produced at leading order in  $\frac{1}{N_c^2}$ . In the latter case one is dealing with a colour suppressed phenomenon where there is an important difference between the probabilistic exclusive (e.g. Lund string) picture and the interference inclusive (perturbative QCD) treatment of the final state particle distributions [2, 4, 9]. Within the inclusive perturbative QCD scenario, in which the interference between radiative amplitudes is fully taken into account, the presence of the different octet and singlet colour states for the  $gg$  system most likely leads to small (i.e. of order  $\frac{1}{N_c^2}$ ) anisotropies in the particle distributions rather than to the appearance of distinctive rapidity gap events with small  $O(\frac{1}{N_c^2})$  probability. In other words, the colour singlet  $gg$  configuration would correspond to an ‘accidental singlet’ [4] with no obvious probabilistic interpretation: additional gluon radiation would ‘smear out’ the colour structure on an event-by-event basis. On the other hand, one might expect that these colour singlet pair events *would* manifest themselves on an event-by-event basis when the invariant masses of the dijet systems are sufficiently small, in which case non-perturbative dynamics (like string formation in the Lund model) would be the dominant effect. This would correspond to two ultra-relativistic small colour dipoles receding from each other with high velocities, too far apart to interact. In the present study, analogously to Refs. [15, 17], we will adopt the latter (probabilistic exclusive) scenario for the final state structure of the  $q\bar{q}gg$  events.<sup>5</sup>

---

<sup>5</sup>For a recent comprehensive discussion of the above colour connection phenomena in processes such as  $e^+e^- \rightarrow q\bar{q}g\dots g$  see Ref. [23].

### 3 Results

In this section we quantify the relative importance of the signal and background contributions in the production of rapidity gap events at LEP2. For the numerical calculations we take  $\alpha_{em} = 1/128$  and  $\sin^2 \theta_W = 0.23$ , while for the  $Z^0$  and  $W^\pm$  boson masses and widths we use the values  $M_{Z^0} = 91.1$  GeV,  $M_W = 80.0$  GeV, and  $\Gamma_{Z^0} = 2.5$  GeV,  $\Gamma_W = 2.2$  GeV. The final-state quarks are taken to be massless. The strong coupling constant  $\alpha_s$  is computed at the two-loop level, with five active quark flavours, at a scale equal to the collider energy  $\sqrt{s}$  and with  $\Lambda_{QCD} = 190$  MeV.<sup>6</sup> The analysis is performed at the parton level, neglecting the effects of hadronization.

In order to be consistent with the experimental procedure of selecting 4-jet final states, we need to adopt a jet-finding algorithm. We choose the ‘Durham’ scheme [24], which uses the clustering variable

$$y_{ij}^D = \frac{2 \min(E_i^2, E_j^2)(1 - \cos \theta_{ij})}{s}, \quad (8)$$

where  $E_i$  and  $E_j$  are the energies of the  $i$ -th and  $j$ -th particle (with four-momenta  $p_i$  and  $p_j$ ), respectively, and  $\theta_{ij}$  their relative angle. A 4-jet event is then defined by requiring that all  $y_{ij}$ ’s (obtained from all possible permutations of  $i$  and  $j$ ) satisfy the condition  $y_{ij} \geq y_{cut}^D = 0.0015$ . None of the main features of our results depend significantly on the jet-clustering procedure and/or on the exact value of  $y_{cut}$ .

Our results are presented in Table I and in Figs. 5–8. In Table I (upper section) we present the total cross sections for the four processes  $e^+e^- \rightarrow W^+W^- \rightarrow q\bar{q}Q\bar{Q}$ ,  $e^+e^- \rightarrow q\bar{q}gg$ ,  $e^+e^- \rightarrow q\bar{q}Q\bar{Q}$  (via  $g$ -propagators), and  $e^+e^- \rightarrow q\bar{q}Q\bar{Q}$  (via  $\gamma, Z^0$ -propagators), for  $y_{cut}^D = 0.0015$  and  $\sqrt{s} = 180$  GeV. These correspond to the ‘fully coloured’ matrix elements in that both colour singlet and octet contributions are included.<sup>7</sup> In computing these cross sections we have summed (averaged) over the final (initial) state helicities and summed over all possible combinations of quark flavours in the final states. For the processes under consideration, quark masses can safely be neglected.

---

<sup>6</sup>In principle, the natural scale for the strong coupling constant  $\alpha_s$  is the characteristic momentum transfer, in which case the effective value of  $\alpha_s$  should be somewhat larger than  $\alpha_s(\sqrt{s})$  due to the lower values of the momenta. However, in what follows we shall treat  $\alpha_s$  as a constant ( $\approx 0.105$ ).

<sup>7</sup>All the results for process (3) presented here neglect gluon radiation and cascading effects and, therefore, are intended only for illustrative purposes – see the discussion at the end of this section.

Since  $2M_W < \sqrt{s} < 2M_{Z^0}$  the cross section for the four-quark process mediated by the double  $W^\pm$  resonance (i.e.  $e^+e^- \rightarrow W^+W^- \rightarrow q\bar{q}Q\bar{Q}$ ) is much larger than the EW  $e^+e^- \rightarrow q\bar{q}Q\bar{Q}$  which includes diagrams with a double  $Z^0$  resonance.<sup>8</sup> Even though the two-gluon QCD process  $e^+e^- \rightarrow q\bar{q}gg$  is produced via  $\gamma^*, Z^0$   $s$ -channel exchange, giving a  $1/s$  suppression, the corresponding 4-jet cross section is comparable to that for  $e^+e^- \rightarrow W^+W^- \rightarrow q\bar{q}Q\bar{Q}$ . Finally, the QCD  $e^+e^- \rightarrow q\bar{q}Q\bar{Q}$  cross section is comparable to that for  $e^+e^- \rightarrow q\bar{q}Q\bar{Q}$  via EW interactions,<sup>9</sup> and roughly an order of magnitude smaller than the cross section for processes (3) and (4), see also Ref. [16].

Figure 5 shows the corresponding differential distribution  $d\sigma/dE_j$  of the energy of a single jet in the four processes, for the above values of  $\sqrt{s}$  and  $y_{cut}^D$ . The symmetry of the matrix elements under interchange of the (anti)quark labels means that the energy distributions are identical for all (massless) partons in the  $e^+e^- \rightarrow W^+W^- \rightarrow q\bar{q}Q\bar{Q}$  and (QCD and EW)  $e^+e^- \rightarrow q\bar{q}Q\bar{Q}$  processes. In contrast, the distributions are *different* for the quarks and gluons in  $e^+e^- \rightarrow q\bar{q}gg$  production. The infrared singularities in gluon bremsstrahlung off quarks in  $q\bar{q}gg$  production lead to a softer energy distribution for the gluons. Another notable feature in Fig. 5 is the peak around  $E_j = 1/4\sqrt{s}$  for  $e^+e^- \rightarrow W^+W^- \rightarrow q\bar{q}Q\bar{Q}$  events, due to the fact that for  $\sqrt{s} \approx 2M_W$  the energy of the quarks from  $W^\pm$  decays is approximately  $M_W/2 \approx 1/4\sqrt{s}$ . The spread of the distribution in Fig. 5 about this value is due mainly to the kinetic energy of the  $W^\pm$  bosons at this above-threshold collision energy. A similar effect is observed in the EW  $e^+e^- \rightarrow q\bar{q}Q\bar{Q}$  distribution, due to the double  $Z^0$ -resonance contribution. Here, however, the additional presence (see Fig. 3a) of  $\gamma^* \rightarrow q\bar{q}$  propagators with soft singularities tends to shift the energy to small values. Finally, the energy distribution of QCD  $e^+e^- \rightarrow q\bar{q}Q\bar{Q}$  events peaks at the edges of the range, since in these events we have quarks both from  $Z^{0*}$  decays with virtuality  $\sqrt{s}$  (and thus  $E_j \approx \sqrt{s}/2$ ) and from soft virtual gluons (i.e. with  $E_j \rightarrow 0$ ).

In order to study colour rearrangement in 4-jet production at LEP2 we are interested in large thrust events in which all jets have approximately the same energy [5]. In Fig. 6 we therefore show the differential thrust distribution  $d\sigma/dT$  for  $y_{cut}^D = 0.0015$ , and with

<sup>8</sup>Increasing or decreasing the value of  $\sqrt{s}$  will, of course, lead to a different relative weighting of these processes. Our choice here of  $\sqrt{s} = 180$  GeV corresponds to maximising the number of  $W^+W^-$  events while remaining below the nominal  $Z^0Z^0$  threshold.

<sup>9</sup>This is true for the particular value of  $y_{cut}$  chosen here. The absolute rates are quite sensitive to the  $y_{cut}$  value, but much of this sensitivity disappears when further kinematical cuts and colour-singlet selections are applied, see below.

an ‘equal energy’ cut, viz.  $|E_j - \sqrt{s}/4| < 10$  GeV for all final-state jets. All colour combinations are again included. The distributions are quite flat for processes (3), (5) and (6) for  $0.7 \lesssim T \lesssim 0.9 - 0.95$ , decreasing as  $T \rightarrow 1$  due to the finite  $y_{cut}^D$  cut. For the processes which are mediated by two virtual massive bosons ( $W^+W^-$  or  $Z^0Z^0$ ) the jets are roughly isotropic in phase space since the collision energy is not far from threshold. For the contribution to (6) in which the  $q\bar{q}Q\bar{Q}$  are produced via intermediate photons, we expect large thrust events when  $\gamma^* \rightarrow q\bar{q}$  propagators have small invariant masses (i.e. collinear  $q$  and  $\bar{q}$ ). This happens in  $\gamma^*\gamma^*$  back-to-back events from the diagrams in Fig. 3b, in  $3 + 1$  back-to-back configurations (i.e. with three collinear jets in one hemisphere) in  $\gamma^*Z^{0*}$  events from Fig. 3b, and in the QCD-like diagrams of Fig. 3a. Since these latter graphs apply also to  $g^* \rightarrow q\bar{q}$ , the same comments hold for process (5). In contrast, the thrust distribution for the QCD process (4) increases significantly at large  $T$ , due to the collinear singularities of the matrix element. For example, a single gluon bremsstrahlung from each of the two quarks gives a back-to-back  $2 + 2$  configuration, while a gluon splitting into a  $gg$ -pair via a triple gluon vertex gives a  $3 + 1$  configuration.

Since our aim is to predict the relative contributions of processes (3)–(6) to 4-jet events with large rapidity gaps and to study colour rearrangement effects, and since these latter occur between parton pairs in colour singlet states (i.e.  $q\bar{q}$ ,  $q\bar{Q}$ ,  $Q\bar{Q}$ ,  $Q\bar{q}$  or  $gg$ ) sufficiently close in phase space, we show in Fig. 7 the distribution in the angular separation  $\cos\theta_S$  between all possible parton pairs which can give such colour singlet configurations. In process (3) singlet states can occur both in  $[q\bar{q}][Q\bar{Q}]$  (both quark and antiquark from the same  $W$ ) and in  $[q\bar{Q}][Q\bar{q}]$  (quark and antiquark from different  $W$ ’s) combinations. For the former, the distribution is peaked in the back-to-back direction (the  $W$ ’s are only slowly moving at this collision energy) whereas the latter distribution is much flatter. Near  $\cos\theta_S = 1$  the distribution is suppressed by the  $y_{cut}^D$  cut. For the QCD  $q\bar{q}gg$  process (4) only  $q\bar{q}$  and  $gg$  pairs can give colour singlet states. The peak in the distributions at  $\cos\theta_S \rightarrow -1$  for both of these combinations reflects the dominance of the back-to-back configuration of the  $q\bar{q}$  pair in the centre-of-mass frame, with gluons preferentially emitted along the quark and antiquark directions. For  $\cos\theta_S \rightarrow 1$  we see a small increase for the  $gg$  distribution due to the collinear singularity in the  $g^*$  propagator splitting into  $gg$ -pairs. The distribution in  $\cos\theta_S$  for the QCD  $q\bar{q}Q\bar{Q}$  process (5)<sup>10</sup> is also strongly peaked in the back-to-back direction. Finally, the  $q\bar{q}$  distribution of the EW  $q\bar{q}Q\bar{Q}$  process (6) has

---

<sup>10</sup>Note that only the  $[q\bar{Q}][Q\bar{q}]$  combination can give a colour singlet here.

almost the same features as that of process (3), apart from the stronger peaking peak at  $\cos\theta_S \rightarrow -1$  which reflects the fact that the  $Z^0Z^0$  pairs are produced almost at rest at this collision energy. As for  $e^+e^- \rightarrow W^+W^- \rightarrow q\bar{q}Q\bar{Q}$ , the distribution for  $q\bar{Q}$  is again quite flat.

The total cross sections corresponding to Figs. 6–7 are listed in Table I (central section), for the same choice of cuts and colour factors. Because of the jet energy dependence of processes (4)–(5) (see Fig. 5), their overall rates are much smaller compared to the other two which are ‘energy resonant’ in the region  $E_j \approx \sqrt{s}/4$ .

The final plot, Fig. 8, shows the thrust dependence of those events which can give rapidity gap configurations. Here only the colour singlet part of the matrix elements has been computed and particles forming singlet states have been required to be close in phase space (i.e.  $\cos\theta_S > 0$ ). Note that for processes (3) and (6) both  $[q\bar{q}][Q\bar{Q}]$  and  $[q\bar{Q}][Q\bar{q}]$  colour singlet configurations are included. It is interesting to note that requiring only positive cosines of  $\theta_S$  and singlet colour factors in the matrix elements almost completely eliminates the collinear singular configurations of the QCD 4–jet events which were apparent in Fig. 6. The effect is clearly visible as a decrease in the thrust dependence of these two processes at large  $T$ .

In Table I (lower section) we list the singlet total cross sections of the four processes, for  $y_{cut}^D = 0.0015$ ,  $|E_j - \sqrt{s}/4| < 10$  GeV and  $\cos\theta_S > 0$ , i.e. the integrated distributions of Fig. 8. There is an obvious hierarchy of cross sections:  $q\bar{q}Q\bar{Q}(W^+W^-) \gg q\bar{q}Q\bar{Q}(EW) \gg q\bar{q}Q\bar{Q}, q\bar{q}gg(QCD)$ , the difference in each case being approximately one order of magnitude. If one assumes an integrated luminosity  $\mathcal{L} = 500$  pb $^{-1}$ , only  $e^+e^- \rightarrow W^+W^- \rightarrow q\bar{q}Q\bar{Q}$  production will give a sizeable number of colour reconnection events at LEP2.

We end this section with a word of caution. The estimate of the number of rapidity gap events for process (3) based on the above four–parton results almost certainly overestimates the size of the colour rearrangement effects. It corresponds to the so–called ‘instantaneous reconnection scenario’ (analogous to Ref. [8]), in which the colour singlet ( $q\bar{Q}$ ) and ( $Q\bar{q}$ ) states are instantaneously formed and allowed to radiate perturbative gluons. It was first shown in Ref. [4] that the finite  $W$  width leads to a space–time separation between the  $W$ ’s, and a consequent additional suppression (by at least an order of magnitude) of the recoupling effects. Therefore the rate of ‘short string’ or rapidity gap production corresponding to processes (3) and (6) may well be of the same order. However the low

overall event rate will surely make these difficult to identify experimentally.

## 4 Conclusions

One of the most important uncertainties in the direct reconstruction method of determining the  $W$  mass from  $q\bar{q}Q\bar{Q}$  events at LEP2 is related to the relatively unknown QCD interconnection effects [4, 5, 6, 7]. To obtain information about the size of these effects it was proposed in Ref. [5] to study the ‘short string’ states signal in  $W^+W^-$  hadronic events in which colour singlet states are formed from  $q\bar{Q}$  and  $Q\bar{q}$  pairs with small phase-space separation. However, such configurations can also be generated by the conventional background  $e^+e^- \rightarrow 4$  parton events in kinematic configurations corresponding to rapidity gap events [14, 15, 16, 17]. In this paper we have presented quantitative estimates of the expected rate from these background processes, including not only the QCD four-parton processes but also the non-resonant electroweak  $q\bar{q}Q\bar{Q}$  processes. In each case we have computed the cross sections corresponding to two pairs of colour singlet partons with modest angular separation and approximately equal parton (jet) energies. We have shown that in this configuration the QCD processes are heavily suppressed, but that electroweak  $q\bar{q}Q\bar{Q}$  production may be comparable in rate to the expected signal from  $W^+W^-$  production.

Finally, we note that aside from their importance to the  $M_W$  measurement at LEP2, rapidity gap events in  $e^+e^-$  annihilation are interesting in their own right as a new laboratory for studying the dynamics of hadron production, see for example Refs. [5, 15, 23]. One of the important issues here is the correspondence between the colour and particle flow dynamics, see for example Ref. [9]. It would be straightforward to extend our calculations to other collider energies and kinematical configurations in order to study such effects.

## Acknowledgements

This work is supported in part by the Ministero dell’ Università e della Ricerca Scientifica, and the EU Programme ‘Human Capital and Mobility’, Network ‘Physics at High Energy Colliders’, contract CHRX-CT93-0357 (DG 12 COMA). VAK, SM and WJS are grateful to the UK PPARC for support. We thank G. Gustafson and T. Sjöstrand for valuable discussions.

## References

- [1] ‘Determination of the Mass of the W Boson’, Z. Kunszt *et al.*, in ‘Physics at LEP2’, eds. G. Altarelli, T. Sjöstrand and F. Zwirner, CERN Report 96-01, Vol.1, p.141-205 (1996).
- [2] For a recent review, see for example: V.A. Khoze in Proc. First Arctic Workshop on Future Physics and Accelerators, Saariselkä, Finland, August 1994, eds. M. Chaichan, K. Huitu and R. Orava, World Scientific, Singapore, 1995, p.458.
- [3] V.S. Fadin, V.A. Khoze and A.D. Martin, *Phys. Rev.* **D49** (1994) 2247; *Phys. Lett.* **B320** (1994) 141.
- [4] T. Sjöstrand and V.A. Khoze, *Z. Phys.* **C62** (1994) 281; *Phys. Rev. Lett.* **72** (1994) 28.
- [5] G. Gustafson and J. Häkkinen, *Z. Phys.* **C64** (1994) 659.
- [6] B.R. Webber, ‘Colour reconnection in HERWIG’, talk given at the LEP2 QCD Working Group meeting, CERN, Geneva, Switzerland, May 1995.
- [7] J. Ellis and K. Geiger, *preprint* CERN-TH/95-283 (1995).
- [8] G. Gustafson, U. Petterson and P.M. Zerwas, *Phys. Lett.* **B209** (1988) 90.
- [9] Yu.L. Dokshitzer, V.A. Khoze, A.H. Mueller and S.I. Troyan, ‘Basics of Perturbative QCD’, ed. J. Tran Thanh Van, Editions Frontieres, Gif-sur-Yvette, 1991; *Rev. Mod. Phys.* **60** (1988) 373.
- [10] B. Andersson, G. Gustafson, G. Ingelman and T. Sjöstrand, *Phys. Rep.* **97** (1983) 31.
- [11] Ya.I. Azimov, Yu.L. Dokshitzer, V.A. Khoze and S.I. Troyan, *Phys. Lett.* **B165** (1985) 147.
- [12] Yu.L. Dokshitzer, V.A. Khoze and S.I. Troyan, *Sov. J. Nucl. Phys.* **50** (1990) 505.
- [13] L. Lönnblad and T. Sjöstrand, *Phys. Lett.* **B351** (1995) 293.
- [14] J. Randa, *Phys. Rev.* **D21** (1980) 1795.
- [15] J.D. Bjorken, S.J. Brodsky and H.J. Lu, *Phys. Lett.* **B286** (1992) 153.

- [16] H.J. Lu, S.J. Brodsky and V.A. Khoze, *Phys. Lett.* **B312** (1993) 215.
- [17] J. Ellis and D.A. Ross, *Z. Phys.* **C70** (1996) 115.
- [18] A. Ballestrero and E. Maina, *Phys. Lett.* **B350** (1995) 225.
- [19] A. Ballestrero, E. Maina and S. Moretti, *Phys. Lett.* **B294** (1992) 425.
- [20] A. Ballestrero, E. Maina and S. Moretti, *Nucl. Phys.* **B415** (1994) 265.
- [21] A. Ballestrero, E. Maina and S. Moretti, *University of Torino preprint DFTT 14/94*, (1994), to be published in Proc. XXIXth Rencontres de Moriond, Méribel, Savoie, France, March 1994.
- [22] R. Kleiss and W.J. Stirling, *Nucl. Phys.* **B262** (1985) 235.
- [23] C. Friberg, G. Gustafson and J. Häkkinen, *University of Lund preprint LU-TP-96-10* (1996).
- [24] S. Catani, Yu.L. Dokshitzer, M. Olsson, G. Turnock and B.R. Webber, *Phys. Lett.* **B269** (1991) 432;  
N. Brown and W.J. Stirling, *Z. Phys.* **C53** (1992) 629.



## Table Caption

- [1] Total cross sections for the four processes: (i)  $e^+e^- \rightarrow W^+W^- \rightarrow q\bar{q}Q\bar{Q}$ , (ii)  $e^+e^- \rightarrow q\bar{q}gg$ , (iii)  $e^+e^- \rightarrow q\bar{q}Q\bar{Q}$  (QCD), (iv)  $e^+e^- \rightarrow q\bar{q}Q\bar{Q}$  (EW), at  $\sqrt{s} = 180$  GeV, for  $y_{cut}^D = 0.0015$ : with complete matrix elements and no additional kinematical cuts (upper section); with complete matrix elements and with the additional cut  $|E_j - \sqrt{s}/4| < 10$  GeV (central section); and with only the ‘singlet’ component of the matrix elements and with the cuts  $|E_j - \sqrt{s}/4| < 10$  GeV and  $\cos\theta_S > 0$  (lower section). Note that for processes (3) and (6) both  $[q\bar{q}][Q\bar{Q}]$  and  $[q\bar{Q}][Q\bar{q}]$  colour singlet configurations are included.

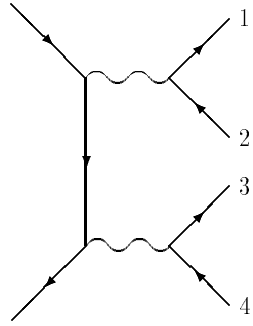
## Figure Captions

- [1] Feynman diagrams contributing in lowest order to  $e^+e^- \rightarrow W^+W^- \rightarrow q\bar{q}Q\bar{Q}$ . A wavy line represents a  $\gamma$ , a  $Z^0$  or a  $W^\pm$ , as appropriate. External lines are identified by their indices as given in the text.
- [2] Feynman diagrams contributing in lowest order to  $e^+e^- \rightarrow q\bar{q}gg$ . A wavy line represents a  $\gamma$  or a  $Z^0$  while the helical line represents a  $g$ . External lines are identified by their indices as given in the text.
- [3] Feynman diagrams contributing in lowest order to  $e^+e^- \rightarrow q\bar{q}Q\bar{Q}$  via QCD (a) and via EW (a and b). If the two quark pairs have different flavour only the first four diagrams in Fig. 3a and the first two in Fig. 3b contribute. A wavy line represents a  $\gamma$  or a  $Z^0$  while a jagged line represents a  $g$ , a  $\gamma$  or a  $Z^0$ , as appropriate. External lines are identified by their indices as given in the text.
- [4] Four-parton mechanisms for generating rapidity gap events in processes (3)–(6). The dashed lines indicate that the produced partons are in colour singlet states: (a) a quark–antiquark jet pair and a two–gluon jet pair; (b) two final quark–antiquark jet pairs produced via QCD interactions; (c) and (d) two final quark–antiquark jet pairs produced via EW interactions.
- [5] Differential distribution  $d\sigma/dE_j$  in the energy of the jet(s) for the four processes: (i)  $e^+e^- \rightarrow W^+W^- \rightarrow q\bar{q}Q\bar{Q}$  (continuous line), (ii)  $e^+e^- \rightarrow q\bar{q}gg$  (dashed line), (iii)  $e^+e^- \rightarrow q\bar{q}Q\bar{Q}$  (QCD) (dotted line), and (iv)  $e^+e^- \rightarrow q\bar{q}Q\bar{Q}$  (EW) (chain–dashed line), at  $\sqrt{s} = 180$  GeV, for  $y_{cut}^D = 0.0015$ . The complete matrix elements are used.
- [6] Differential distribution  $d\sigma/dT$  in thrust for the four processes: (i)  $e^+e^- \rightarrow W^+W^- \rightarrow q\bar{q}Q\bar{Q}$  (continuous line), (ii)  $e^+e^- \rightarrow q\bar{q}gg$  (dashed line), (iii)  $e^+e^- \rightarrow q\bar{q}Q\bar{Q}$  (QCD) (dotted line), and (iv)  $e^+e^- \rightarrow q\bar{q}Q\bar{Q}$  (EW) (chain–dashed line), at  $\sqrt{s} = 180$  GeV, for  $y_{cut}^D = 0.0015$  and  $|E_j - \sqrt{s}/4| < 10$  GeV. The complete matrix elements are used.

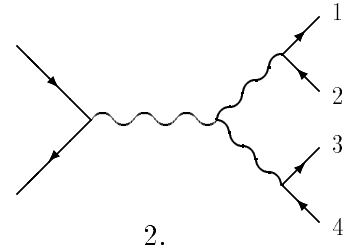
- [7] Differential distribution  $d\sigma/d\cos\theta_S$  in the cosine of the ‘singlet angle’ for the four processes: (i)  $e^+e^- \rightarrow W^+W^- \rightarrow q\bar{q}Q\bar{Q}$  (continuous line), (ii)  $e^+e^- \rightarrow q\bar{q}gg$  (dashed line), (iii)  $e^+e^- \rightarrow q\bar{q}Q\bar{Q}$  (QCD) (dotted line), and (iv)  $e^+e^- \rightarrow q\bar{q}Q\bar{Q}$  (EW) (chain-dashed line), at  $\sqrt{s} = 180$  GeV, for  $y_{cut}^D = 0.0015$  and  $|E_j - \sqrt{s}/4| < 10$  GeV. The complete matrix elements are used.
- [8] Differential distribution  $d\sigma/dT$  in thrust for the four processes: (i)  $e^+e^- \rightarrow W^+W^- \rightarrow q\bar{q}Q\bar{Q}$  (continuous line), (ii)  $e^+e^- \rightarrow q\bar{q}gg$  (dashed line), (iii)  $e^+e^- \rightarrow q\bar{q}Q\bar{Q}$  (QCD) (dotted line), and (iv)  $e^+e^- \rightarrow q\bar{q}Q\bar{Q}$  (EW) (chain-dashed line), at  $\sqrt{s} = 180$  GeV, for  $y_{cut}^D = 0.0015$ ,  $|E_j - \sqrt{s}/4| < 10$  GeV and  $\cos\theta_S > 0$ . Only singlet components of the matrix elements were used. Note that for processes (3) and (6) both  $[q\bar{q}][Q\bar{Q}]$  and  $[q\bar{Q}][Q\bar{q}]$  colour singlet configurations are included.

$\sigma$ (pb)			
$W^+W^- \rightarrow q\bar{q}Q\bar{Q}$	$q\bar{q}gg$	$q\bar{q}Q\bar{Q}$ (QCD)	$q\bar{q}Q\bar{Q}$ (EW)
6.34	4.33	0.240	0.186
no kinematical cuts		singlet+octet	
1.32	$6.84 \times 10^{-2}$	$1.06 \times 10^{-3}$	$4.75 \times 10^{-2}$
$ E_j - \sqrt{s}/4  < 10$ GeV		singlet+octet	
$2.54 \times 10^{-2}$	$5.16 \times 10^{-5}$	$9.44 \times 10^{-5}$	$3.01 \times 10^{-3}$
$ E_j - \sqrt{s}/4  < 10$ GeV		$\cos\theta_S > 0$	singlet only

Table I



1.



2.

**Fig. 1**

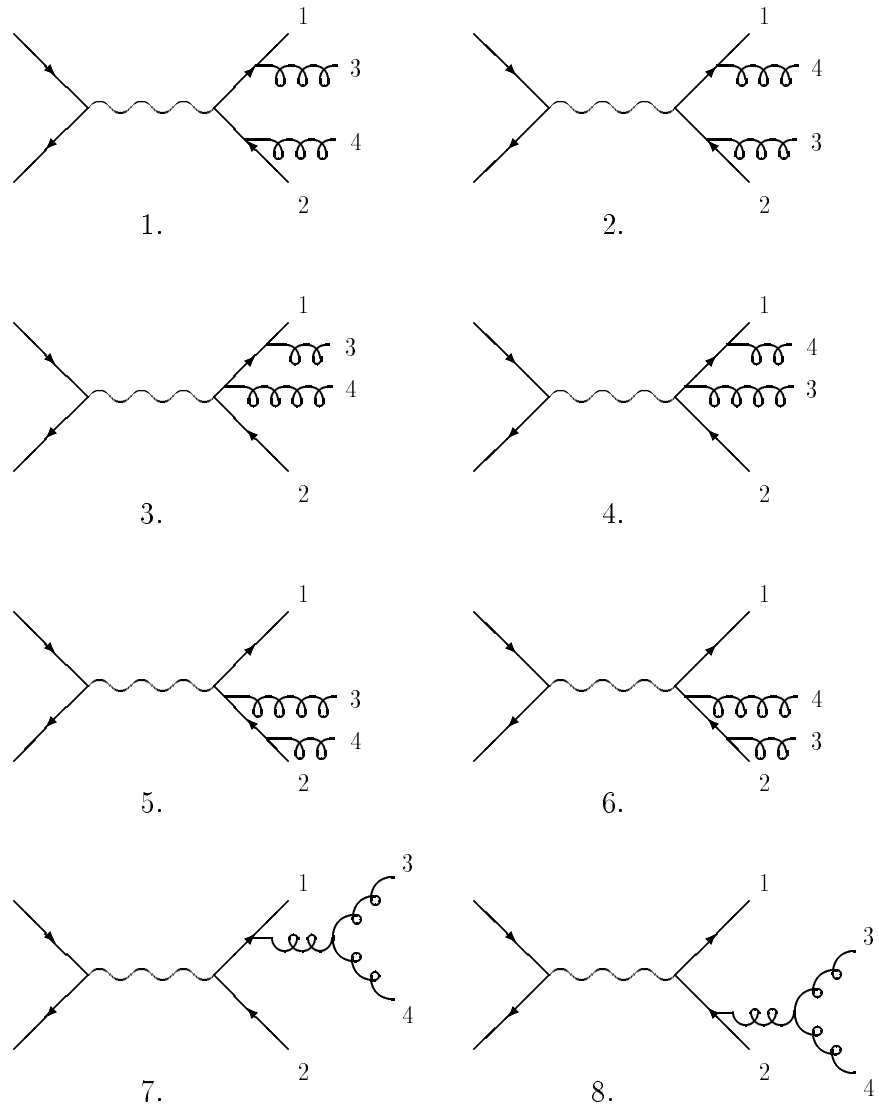


**Fig. 2**

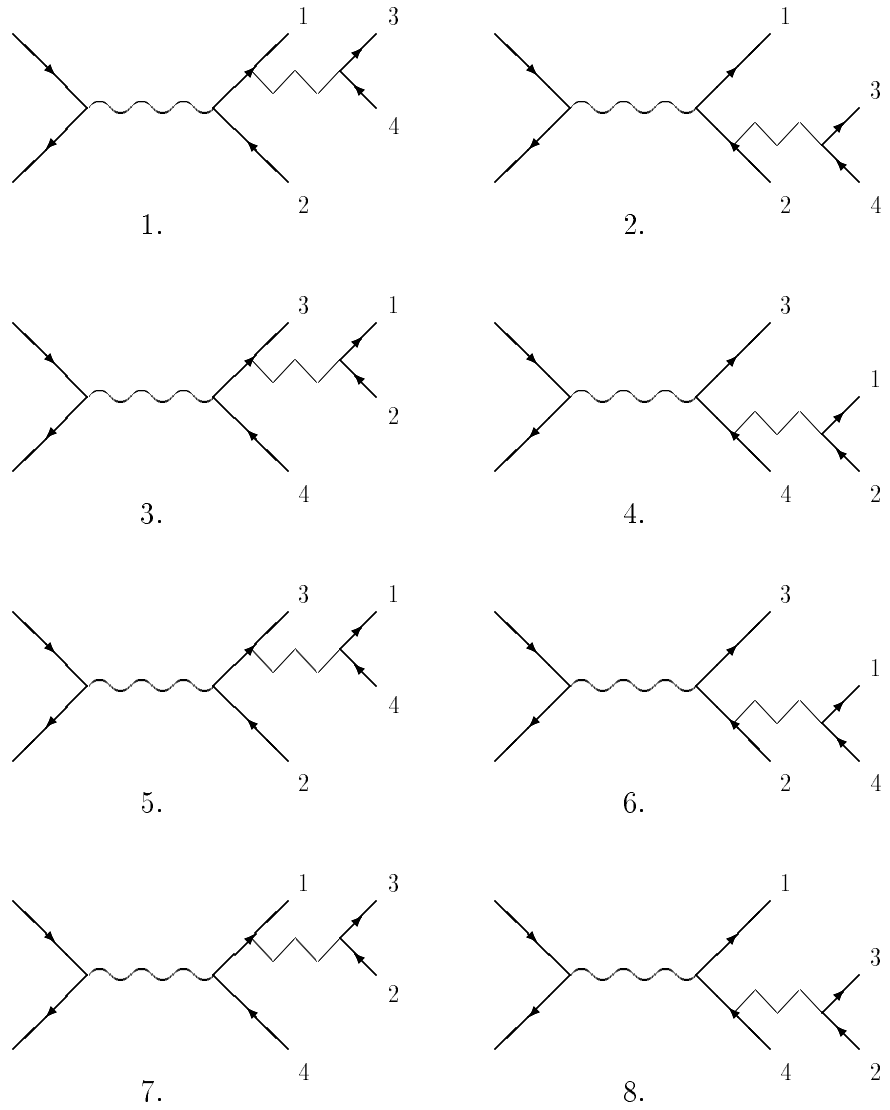
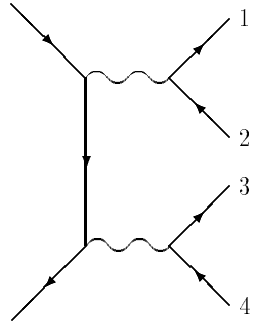
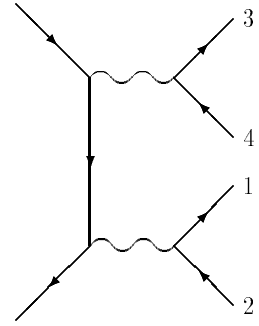


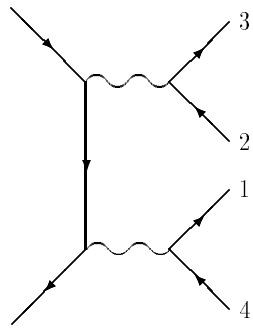
**Fig. 3a**



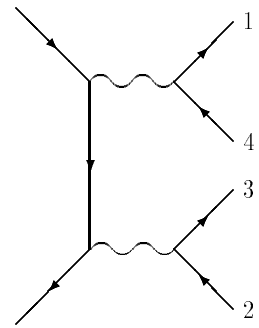
5.(9.)



6.(10.)



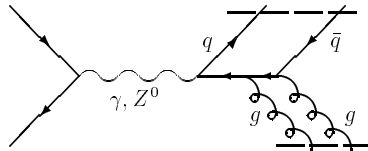
(11.)



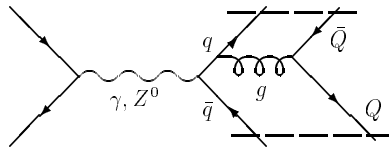
(12.)

**Fig. 3b**

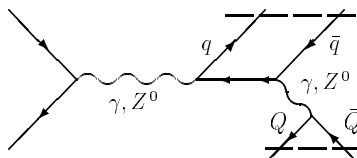




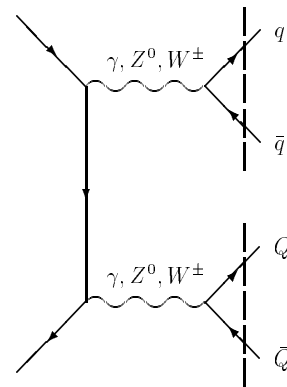
(a)



(b)



(c)



(d)

**Fig. 4**

$e^+ e^- \rightarrow jjjj$  at LEP 2

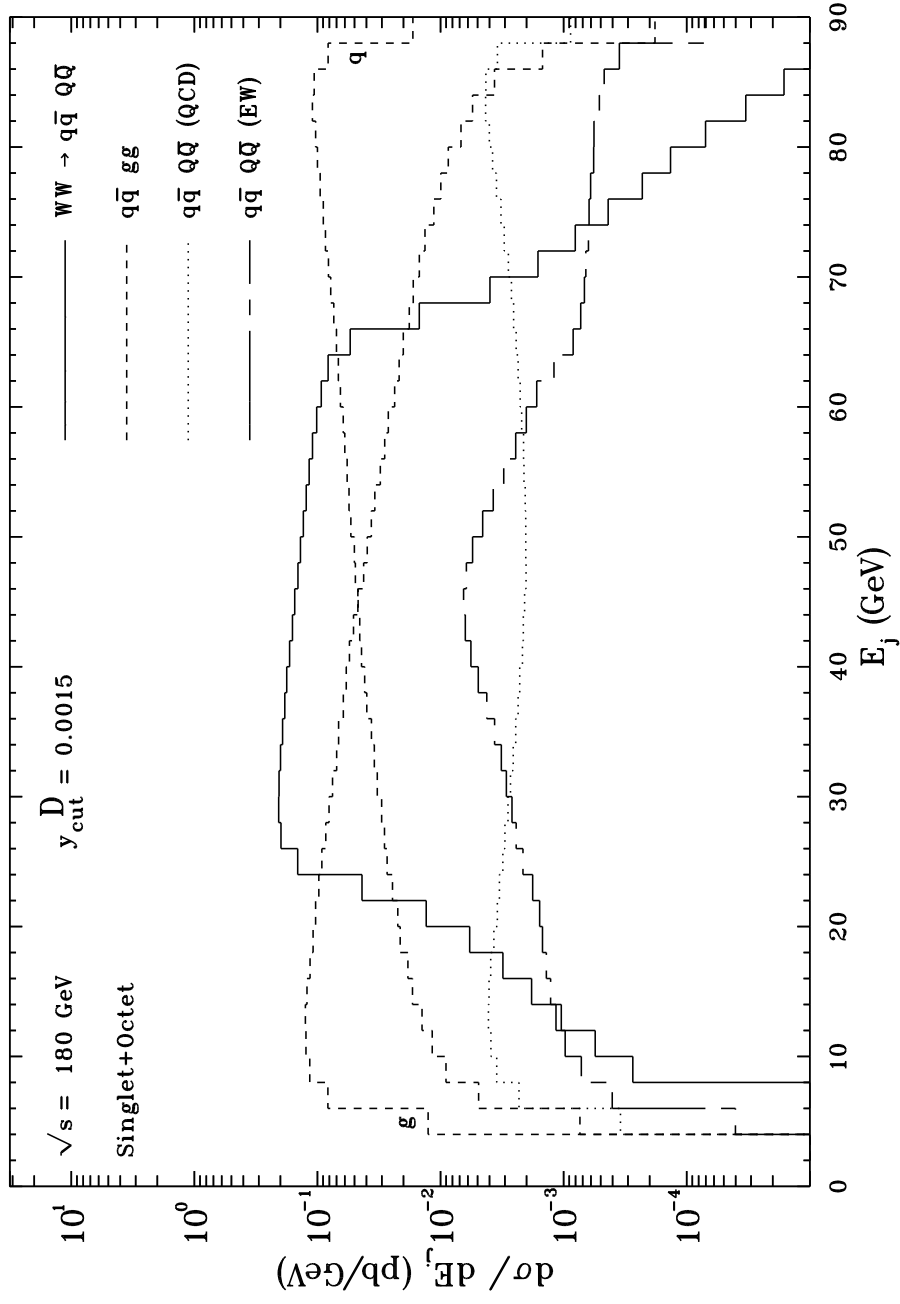


Fig. 5

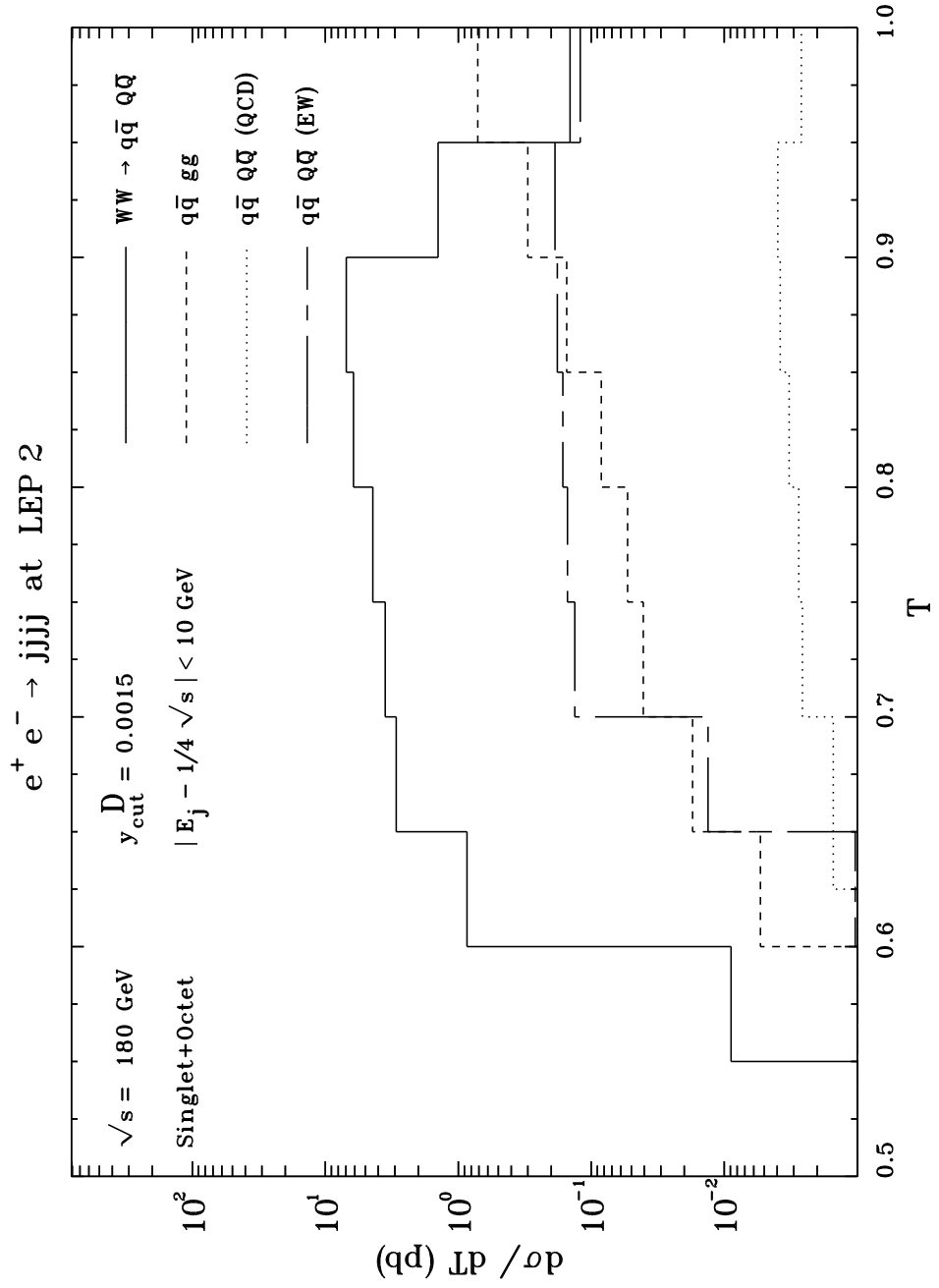


Fig. 6

$e^+ e^- \rightarrow jjjj$  at LEP 2

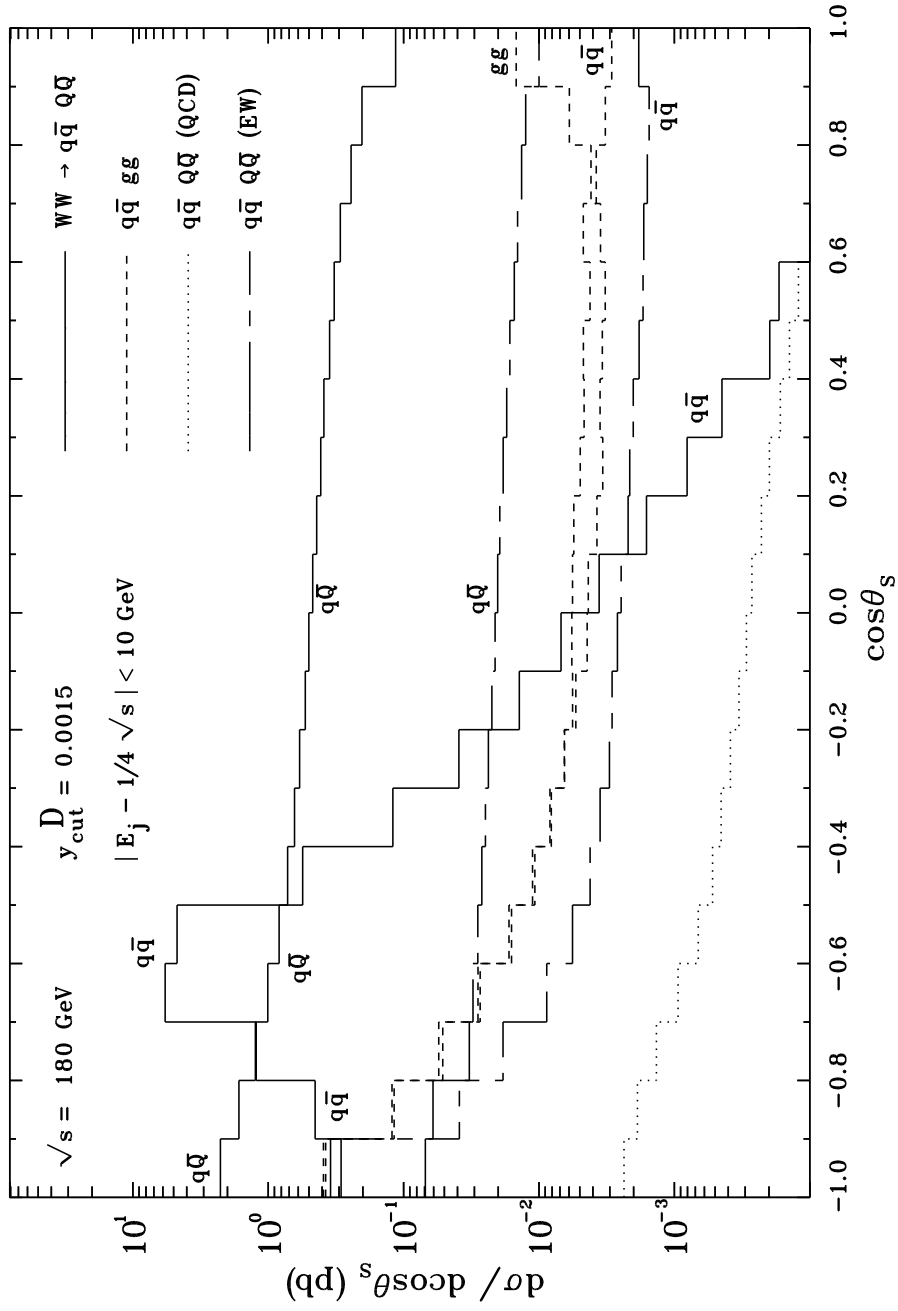


Fig. 7

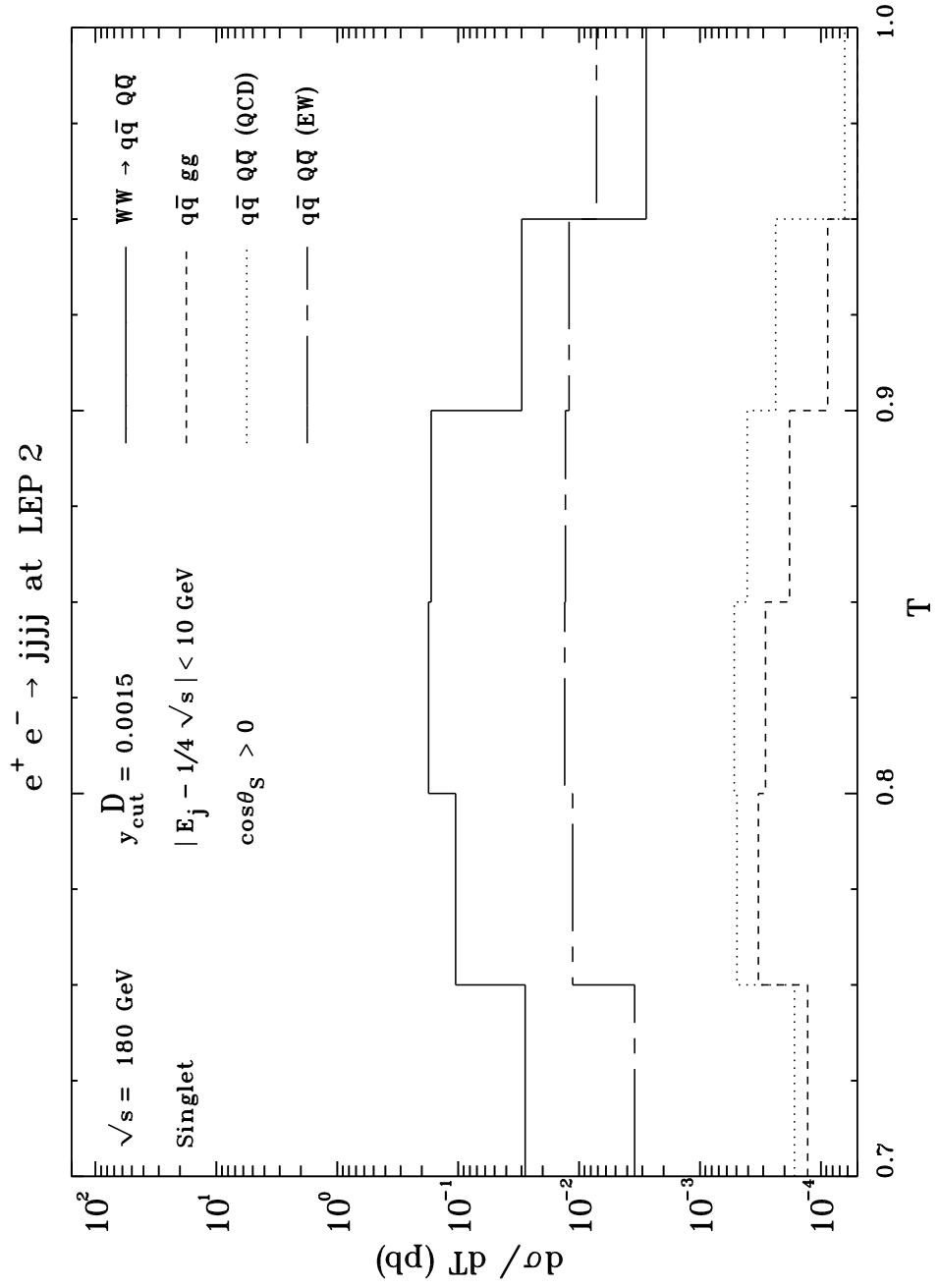


Fig. 8